Obtaining sub-daily new snow density from automated measurements in high mountain regions

Kay Helfricht[1], Lea Hartl[1], Roland Koch[2], Christoph Marty[3], Marc Olefs[2]

[1]IGF - Institute for Interdisciplinary Mountain Research, Austrian Academy of Sciences, Innsbruck, 6020, Austria
[2]ZAMG - Zentralanstalt für Meteorologie und Geodynamik, Climate research department, Vienna, Austria
5 [3]WSL Institute for Snow and Avalanche Research SLF, Davos, Switzerland

Correspondence to: Kay Helfricht (kay.helfricht@oeaw.ac.at)

Abstract. The density of new snow is operationally monitored by meteorological or hydrological services at daily time intervals, or occasionally measured in local field studies. However, meteorological conditions and thus settling of the freshly
10 deposited snow rapidly alter the new snow density until measurement. Physically based snow models and now-casting applications make use of hourly weather data to determine the water equivalent of the snowfall and snow depth. In previous studies, a number of empirical parameterizations were developed to approximate the new snow density by meteorological parameters. These parameterizations are largely based on new snow measurements derived from local in-situ measurements. In this study a data set of automated snow measurements at four stations located in the European Alps is analysed for several
15 winter seasons. Hourly new snow densities are calculated from the height of new snow and the water equivalent of snowfall. Considering the settling of the new snow and the old snowpack, the average hourly new snow density is 68 kg m^{-3} with a standard deviation of 9 kg m^{-3}. Seven existing parameterizations for estimating new snow densities were tested against these data, and most calculations overestimate the hourly automated measurements. Two of the tested parameterizations were capable of simulating low new snow densities observed at sheltered inner-alpine stations. The observed variability in new
20 snow density from the automated measurements could not be described with satisfactory statistical significance by any of the investigated parameterizations. Applying simple linear regressions between new snow density and wet bulb temperature based on the measurements data resulted in significant relationships ($r² > 0.5$ and $p \leq 0.05$) for single periods at individual stations only. Higher new snow density was calculated for the highest elevated and most wind exposed station location. Whereas snow measurements using ultrasonic devices and snow pillows are appropriate for calculating station mean new
25 snow densities, we recommend instruments with higher accuracy e.g. optical devices for more reliable investigations of the variability of new snow densities on sub daily intervals.

1 Introduction

In mountain regions there is an increasing demand for high-quality analysis, now-casting and short range forecasts of the
30 spatial distribution of snowfall. Operational services, concerning avalanche warning, road maintenance and hydrology, as

well as hydropower companies and ski resorts need reliable information on the depth of new snow (HN) and the water equivalent (HNW) of snowfall. Therefore the new snow density (ρ_{HN}) is needed to convert HN into HNW and vice versa. Information on HN is especially relevant for cold and windy conditions, when measuring HNW is a difficult task because conventional rain gauge measurements are prone to large errors (e.g. Goodison et al., 1998). Recent results of the Solid Precipitation Intercomparison Experiment (SPICE; Nitu et al., 2012) reveal that these errors still exist in standard meteorological measurements (e.g. Buisan et al., 2016; Pan et al., 2016). Many snow cover models calculate HN from HNW on subdaily time intervals, although reliable HNW input data are difficult to obtain (Egli et al., 2009), and thus the new snow density is needed in equal temporal resolution to convert between HNW and HN (e.g. Lehning et al., 2002; Roebber et al., 2003; Olefs et al., 2013). Additionally, ρ_{HN} has a considerable effect on the snow bulk density of the total snowpack (e.g. Schöber et al., 2016).

Since the 1960s ultrasonic rangers have become more common for observing snow depth changes automatically even on sub-hourly time intervals (e.g. Gubler, 1981; Goodison et al., 1984; Lundberg et al., 2010). They have the advantage of a more objective method compared to subjective manual measurements of snow depth (Ryan et al. 2008). Beside snow depth (HS), the water equivalent of the snowpack (SWE) is observed operationally using weighing devices such as lysimetric snow pillows (e.g. Serreze et al. 2009; Egli et al., 2009; Lundberg et al., 2010; Krajci et al., 2017) and snow scales (e.g. http://www.sommer.at/en/products/snow-ice/snow-scales-ssg). Upward looking GPR (e.g. Heilig et al., 2009), GPS techniques (e.g. Koch et al., 2014; McCreight et al., 2014) and the combination of both (Schmidt et al., 2015) have been applied in scientific studies to monitor the depth, SWE and liquid water content of the snowpack. However, these techniques are rather expensive or not yet in use for long-term observations by operational services. In general, automatic measurements of SWE are prone to a high relative uncertainty and require a certain degree of maintenance, which makes them complex and labour-intensive (Smith et al., 2017). Due to such constrains, SWE measurement instrumentation is installed at considerably fewer stations compared to HS instruments, and only at sites with easy access for appropriate maintenance. Recent studies present the performance of cosmic ray neutron sensors (e.g. Schattan et al., 2017), which partly are used for long-term observations such as e.g. from Col de Porte (Morin et al., 2012).

The density of new snow is influenced by the shape and size of the snow crystals (e.g. Nayaka, 1951). Relationships between predominant snow crystal type, riming properties and snowfall density where already reported by Power et al. (1964) from snowstorm observations in Canada. Once the snow crystals have accumulated at the snow surface, the density of the fresh snow starts to increase depending on prevailing weather conditions and compaction caused by overlaying of snow. A common mean ρ_{HN} used to convert between HN and HNW is 100 kg m^{-3}. Many studies analysed ρ_{HN} values on a daily basis and confirmed this 10:1-rule as applicable for a first estimate (e.g. Roebber et al., 2003; Egli et al., 2009; Teutsch, 2009). However, ρ_{HN} span a wide range and values from 10 to 350 kg m^{-3} have been reported from American and European mountain ranges, with mean values between 70 and 110 kg m^{-3} (e.g. Diamond and Lowry, 1954; LaChapelle, 1962; Power et

al., 1964; Judson, 1965; McKay et al., 1981; Meister, 1985; Judson and Doesken, 2000; Valt et al., 2014). Most of the ρ_{HN} data analysed in these studies were observed using readings on a snow board. The density is calculated from HN measured with a ruler and HNW is derived from an external precipitation device or from weighing the new snow either in solid or melted form (Fierz et al., 2009).

5   Several studies have shown that measured ρ_{HN} can be related to meteorological parameters, although with different time intervals and different degrees of determination. In 1952, Gold and Power showed that the crystal type is related to its estimated formation temperature. Diamond and Lowry (1954) and Simeral et al. (2005) built an empirical calculation that ascertained relationships between ρ_{HN} and air temperature at the 700-mb level. Teutsch (2009) also concluded that ρ_{HN} of 12 hour intervals at valley stations is best correlated to the wet bulb temperature at mountain stations in close vicinity

10   ($r^2 = 0.86$). Judson and Doesken (2000) found that near-surface air temperature and new snow density at mountain stations could explain 52 % of the variance in snow density. Wetzel et al. (2004) presented a similar degree of correlation of ρ_{HN} to temperature at three high-elevation sites. Alcott and Steenburg (2009) showed that ρ_{HN} is correlated with near-crest-level temperature and wind speed particularly for high-SWE events. Wright et al. (2016) presented a statistical analysis of data from 42 seasons of manual daily snow density measurements along with air temperature and wind speed to derive

15   parameterizations to estimate new snow density. However, they end up with a low coefficient of determination.

On the basis of data from 7 stations in Switzerland located between 1250 and 1800 m a.s.l., Meister (1985) concluded that ρ_{HN} does not correlate with the amount of new snow (HN), that it does not depend on altitude, and that air temperature does not accurately determine ρ_{HN}. Nevertheless, binning the data into temperature classes results in a statistical equation with a correlation coefficient of 0.85. Further, he recommended considering wind speed in addition to air temperature, at least for

20   stations higher than 1800 m a.s.l. On the basis of data sets from of Schmidt and Gluns (1991) and the US Army Corps of Engineers (1956), Hedstrom and Pomeroy (1998) developed a power function using the air temperature for which they found a coefficient of determination of 0.84 and a standard error of estimate of 9.3 kg m^{-3}. Jordan et al. (1999) introduced an algorithm for assigning ρ_{HN} within the SNTHERM snow cover model. They added wind dependence to the temperature parameterization of Meister (1985). This achieved a reduction of the error, but a significant scatter remained between

25   observed and parameterized ρ_{HN} values. Lehning et al. (2002) built an empirical calculation for ρ_{HN} valid for a time interval of 30 to 60 minutes in the framework of the snow model SNOWPACK. They used air temperature, surface temperature, relative humidity and wind speed for the regression analysis and achieved an approximate multiple coefficient of determination of 0.83. Schmucki et al. (2014) used another empirical power relation, including air temperature, wind speed and relative humidity, to calculate the ρ_{HN} using SNOWPACK simulations for three contrasting sites in Switzerland. ρ_{HN}

30   were analysed in short time intervals of one to two hours by Ishizaka et al. (2015). They measured even lower densities in comparison to ρ_{HN} estimates obtained using the SNOWPACK density model, especially for aggregated snow crystal types. On the basis of data from Col de Porte (1325m altitude, French Alps), Pahaut et al. (1976) developed a statistical relationship

including the melting point of water, air temperature and wind speed. This parameterization is used to calculate the density of new snow in the snow cover model CROCUS (Vionnet et al., 2012).

Settling of the new snow by its weight and destructive metamorphism may reduce HN and hence increase ρ_{HN} between snowfall and the HN reading and has to be considered when computing new snow density (e.g. Anderson 1976; Lehning et al., 2002; Steinkogler, 2009; Vionnet et al., 2012). The contribution of settling to snow depth changes is highest in the first hours after a snowfall. Wind drift and radiation input to the snow surface after the snowfall may increase ρ_{HN} in comparison to ρ_{HN} at the time of snowfall. However, direct measurements of ρ_{HN} at the time of snowfall are laborious and difficult to align with the hours of peak snowfall rates.

Whereas most of the studies have analysed daily and sub-daily, manual ρ_{HN} measurements, to our knowledge no extensive analysis of automated ρ_{HN} measurements in hourly intervals over several winter seasons exists. The aim of this study is to assess the value of automated measurements of hourly HN and HNW for the calculation of ρ_{HN} at different stations and in hourly time interval. Therefore we examine the following questions:

(1) Are automated measurements of HN and HNW suitable for the calculation of ρ_{HN} at hourly interval?

(2) How do the mean and the variability of observed ρ_{HN} differ between distinct study sites?

(3) How well do established density parametrisations represent observed hourly ρ_{HN} values?

To this end, we calculated ρ_{HN} from hourly snow depth changes (HN) and hourly SWE changes (HNW). The mean values and the variability of hourly ρ_{HN} are discussed for observations at four different meteorological stations and compared to calculations using established ρ_{HN} parameterizations. A critical assessment with outlook on next generation measurements techniques is given in the discussion.

2 Data and Methods

Data from four automatic weather stations (AWS) were used in this study (Fig. 1, Table 1). A prerequisite for the station selection was the combined measurement of HS and SWE at each station in addition to the standard meteorological measurements of air temperature, relative humidity, precipitation, wind speed and global radiation. HS data are measured using ultrasonic rangers. SWE data are recorded using snow pillows. Details regarding the instruments at and the exact location of each AWS, as well as the start and end dates of the available data coverage are presented in Table 1.

The Kühroint station (Germany) is operated by the Bavarian Avalanche Warning Service. It is a well-equipped and maintained station for snow climate at the northern fringe of the Eastern Alps. It is located in a meadow below treeline.

The Kühtai station (Austria) is operated by the Tiroler Wasserkraft AG (TIWAG). It is located south of the Inntal valley, but north of the Alpine main ridge, and it is situated at a wind-sheltered location.

The station at Wattener Lizum (Austria) is operated by the Austrian Research Centre for Forests (BFW) of the Federal Ministry of Agriculture, Forestry, Environment and Water Management. This station is situated in a south-north oriented

5   high alpine valley above the treeline near to the Alpine main ridge.

The station at Weissfluhjoch (Switzerland) is operated by the Institute for Snow and Avalanche Research (SLF), which is part of the Swiss Federal Institute for Forest, Snow and Landscape Research (WSL). Weissfluhjoch is the highest elevated station considered in this study.

On the basis of coinciding data availability we consider four time periods as presented in Table 1. Data outputs of the AWS

10   are logged at time intervals ranging from 2 to 30 minutes. Hourly values were computed for global radiation, relative humidity, air temperature and wind speed. The hourly value is the mean of the previous hour. For precipitation it is the sum of the previous hour. To account for noise in the ultrasonic signal, HS and SWE where smoothed using a centred moving average over 3 values in the original data resolution. The hourly values for HS and SWE are the instantaneous values on the full hour from the smoothed time series.

15   The thermodynamic wet bulb temperature (T_w) was computed applying the psychrometric equation (Sonntag, 1990) and an exact iterative approach presented by Olefs et al. (2010). A standard barometric equation was used to determine air pressure based on the station elevation. Air pressure dependency of T_w is generally minor and only relevant for air temperatures larger than +2°C (Olefs et al., 2010).

A necessary condition for all further analysis of the time series was the presence of a precipitation signal at the heated

20   precipitation gauges in combination with positive snow depth changes. Then, the hourly height of new snow (HN) and the water equivalent of snowfall (HNW) were computed as the change in HS and SWE. Within the next filtering step, only HN and HNW values with T_w less than 0°C and a wind speed (u) of less than 5 m s^{-1} were considered.

Constraints have to be made in order to avoid low values of HNW and HN, which are prone to large relative errors due to random and systemic measurement uncertainties in HN and SWE, but a minimum of approx. 100 remaining samples for

25   statistical analysis must be ensured.

To investigate the influence of different minimum HNW and HN limits, a distribution matrix was calculated by varying the minimum HNW and HN limits in steps of 0.5 mm for HNW and 0.5 cm for HN, respectively. To account for settling during ongoing snowfall, the compaction correction described in Anderson (1976) was applied. The approach was simplified with respect to HS, SWE and snow density by considering only two layers of the snowpack: the new snow and the total snowpack

30   of the previous time step. Destructive settling (S) of HN is considered for each time step where the snow depth increases (Eq. 1). The destructive settling of the new snow (S_{HN}) for each time step is calculated by

$$S_{\mathrm{HN}} = -0.000002777 \cdot e^{(0.04 \cdot T)} \qquad \{\rho_{\mathrm{HN}} \leq 150\ kg\ m^{-3}\} \tag{1a}$$

$$S_{\mathrm{HN}} = S_{\mathrm{HN}} \cdot e^{(0.046 \cdot T \cdot (\rho_{\mathrm{HN}} - 150))} \qquad \{\rho_{\mathrm{HN}} \geq 150\ kg\ m^{-3}\}, \tag{1b}$$

where T is the air temperature. Settling of the new snow layer caused by the weight of the ongoing snow accumulation is not taken into account.

Settling within the old snowpack is computed considering the total snow depth (HS). The destructive settling within the old snow layer (S_{HS}) is calculated using Eq. (1), substituting HS for HN and using the bulk density of the old snowpack (ρ_{HS}) calculated from HS and total SWE of the previous time step. Settling within the old snowpack caused by the weight of the snowpack (S_{wHS}) is given as:

$$S_{\mathrm{wHS}} = -248.976 \cdot \frac{HN}{3600000} \cdot e^{0.8 \cdot T} \cdot e^{-0.021 \cdot \rho_{\mathrm{HS}}}. \tag{2}$$

The resulting settling factors of S_{HN}, S_{HS} and S_{wHS} are multiplied with HS and HN to adjust HN accordingly.

New snow density (ρ_{HN}) was obtained from the ratio of HN to HNW. Outliers below the 5 % percentile and higher than the 95 % percentile were excluded. The ρ_{HN} data were grouped by wet bulb temperature and wind speed, using bins of 1°C and 0.5 ms^{-1} respectively. A least squares regression was carried out using both the ungrouped data and the median of the grouped data to quantify possible correlations of ρ_{HN} with T_{w} and u.

The ρ_{HN} were compared to the following parameterizations developed in previous studies. In these parametrisations, ρ_{HN} is a function of meteorological parameters such as air temperature (T), wind speed (u) and relative humidity (rH). The time interval for ρ_{HN} readings of the respective study is given in the brackets.

$$\rho_{\mathrm{HP}} = 67.92 + 51.52 \cdot e^{\frac{T}{2.59}} \qquad \text{(Hedstrom and Pomeroy 1998, event/daily)} \tag{3}$$

$$\rho_{\mathrm{D}} = 119 + 6.48\,T \qquad \text{(Diamond and Lowry 1954, frequent interval during event)} \tag{4}$$

$$\rho_{\mathrm{LC}} = 50 + 1.7 \cdot (T + 15)^{1.5} \qquad \text{(LaChapelle 1962, event)} \tag{5}$$

$$\rho_{\mathrm{J}} = 500 \cdot \left(1 - 0.951 \cdot e^{-1.4 \cdot (5-T)^{-1.15} - 0.008 \cdot u^{1.7}}\right) \quad \{-13^\circ\,C < T \leq 2.5^\circ\,C\} \tag{6a}$$

$$\rho_{\mathrm{J}} = 500 \cdot \left(1 - 0.904 \cdot e^{-0.008 \cdot u^{1.7}}\right) \quad \{T \leq 13^\circ\,C\} \qquad \text{(Jordan et al., 1999, event/daily)} \tag{6b}$$

$$\rho_{\mathrm{V}} = 109 + 6 \cdot (T - T_f) + 26\,u^{0.5} \qquad \text{(Vionnet et al., 2012, event/daily)} \tag{7}$$

$$\rho_{\mathrm{S}} = 10^{3.28 + 0.03T - 0.36 - 0.75 \cdot \arcsin(\sqrt{0.01 \cdot rH} + 0.03 \cdot \log_{10} u)} \quad \{T \geq -14^\circ\,C\} \tag{8a}$$

$$\rho_{S} = 10^{3.28 + 0.03T - 0.75 \cdot \arcsin(\sqrt{0.01\,rH} + 0.03 \cdot \log_{10} u)} \quad \{T < -14^{\circ}\,C\} \text{ (Schmucki et al., 2014, event/hourly)} \qquad (8b)$$

$$\rho_{L} = 70 + 6.5\,T + 7.5\,T_s + 0.26\,rH + 13\,u - 4.5\,T\,T_s - 0.65\,T\,u - 0.17\,rH\,u + 0.06\,T\,T_s\,rH \qquad (9)$$

$$\text{(Lehning et al., 2002, event/hourly)}$$

5   The melting point of snow (T_f) in Eq. (7) was approximated as 0°C (Vionnet et al., 2012). Following Schmucki et al. (2014), we limited the parameter range and set *rH* to a constant value of 0.8 (80 %) during snowfall and the lower boundary for the wind speed to 2 ms^{-1}.

The temperature of the snow surface (T_s) is required in Eq. (9). As this was not available for each station, we used the approximation $T_s = T$. We argue that T_s could not considerably exceed 0°, because of the maximum T_w of 0°C. Since only

10   precipitation events are considered, *rH* can be expected to be high, and thus difference between T_w and T is small.

The uncertainty of ultrasonic measurements on snow can be assumed to be in the range of ± 1 cm, which partly is a consequence of changes in signal velocity due to meteorological conditions. However, we used the original HS data logged in mm-resolution to avoid the effects caused by rounding to full cm when calculating HN. Likewise, we used the tenths mm SWE data logged at the pillows. Another documented error source of the HS measurement is signal blocking by e.g. dense

15   snowfall or drifting snow, which causes peaks of the HS. However, with the filtering procedure applied in this study, no such spikes were left in the analysis.

A source of uncertainty is the spatial offset between the HS measurements and the SWE measurements. HS is measured directly above the SWE measurement at Kühtai station, Kühroint station and Wattener Lizum station (Fig. 1). However, the footprint of the snow depth sensor may be smaller than the surface area of the pillow, and it is decreasing with increasing

20   HS. A spatial variability of HS on the pillow can be caused by snow drift and differing snow settling or snow melt.

For the calculations within this study we used the changes in HS and SWE over the time period of snowfall only. Errors due to spatial variability in HS and SWE caused by spatial differences in energy consumption and snow drift between precipitation events are reduced. This is especially valid for the HS and SWE measurements at the stations with matching HS and SWE measurements. The snow depth sensor and the snow pillow of Weissfluhjoch station are separated by 9 meters.

25   Schmid et al. (2014) suggest a small-scale variability in HS of ±4.3 % at the Weissfluhjoch station. Again, the error may be smaller due to using temporally limited changes of HS, but an additional uncertainty of ±5 % can be assumed here.

A well-known issue with snow pillows are bridging effects (e.g. Serreze et al., 1999; Johnson and Schaefer, 2002). Dense snow layers and crusts within the snowpack sustain the weight of the new snow so that HNW, and thus ρ_{HN}, are

30   underestimated. We cannot exclude such data explicitly. However, all filtering conditions have to be fulfilled for including values in the analysis, so that data without or with lagged HN increase were not considered. Additionally, the chosen snow stations are well maintained in case of implausible data due to their overall good accessibility. E.g. trenches are dug out

around the base area of the snow pillow at Kühtai station to cut off the measured part of the snowpack to avoid bridging effects.

Nevertheless, the measurement uncertainty is ± 1cm for HN and 0.1 cm for HNW. Considering mean HN (Table 2) and HNW values, the uncertainty is ± 25 kg m^{-3} or 37 % of the mean density. This value is lower considering higher HN, but increases to 80 % for the combination of minimum HN and minimum HNW of 1.6 cm and 0.2 mm respectively.

3 Results and discussion

3.1 Data filtering, correction of settling and evaluation

Figure (2) presents the median new snow density (ρ_{HN}) data calculated from all filtered HN and HNW exceeding the respective minimum HN and HNW limits. This presentation highlights the variability of ρ_{HN} by using different minimum limits with respect to the high relative uncertainty of low HN and HNW values. Changing the minimum limits for HN and HNW affects the resulting ρ_{HN} considerably. However, increasing the minimum limits for HN and HNW results in a distinct lowering of the number of data remaining for the subsequent analysis (Fig. 2). There are certain differences between the stations for high minimum HNW limits. Calculated ρ_{HN} decrease when low minimum HN and high minimum HNW limits are applied at Kühtai and Wattener Lizum station. In contrast, ρ_{HN} increase for equal minimum limits at Kühroint and Weissfluhjoch station. At Kühtai and Wattener Lizum station, high HNW values of more than 3 mm HNW are accompanied by rather high HN (Fig. 2). In contrast, low HN occurring with high HNW at Kühroint and Weissfluhjoch cause high ρ_{HN}. However, these results are based on a small number of values only. In general, the calculated median ρ_{HN} are rather constant following the 1:1 line of minimum HNW and HN limits (Fig. 2).

In order to avoid low values of HNW and HN, but ensuring an appropriate number of approx. 100 samples and with respect to the results of the Figures 2, we decided to use a minimum limit of 1.5 mm in HNW and 2.0 cm in HN. This leads to the exclusion of on average 94 % of all data points that have a precipitation signal and positive snow depth changes (Table 2). Frequency distributions for HN, HNW, T_w and u of the unfiltered and filtered data are presented for each station and for each time period in the supplement Figures (S01) to (S09).

The exclusion of high wind speeds has only a small effect at the lower stations and is more noticeable at the more wind exposed stations of Wattener Lizum and Weissfluhjoch. Considering period 1 comprising all stations, the filtering process causes the highest filtering rate for Weissfluhjoch station, with 6 % of data remaining after applying the filtering. The overall highest amount of data reduction is found at Kühtai station, with 5 % of the data remaining after filtering of the longer

periods 3 and 4 (Table 2). There was a considerable fraction of data with positive HS changes, a precipitation signal and positive T_w. Most of these data seem to be paired with very small HS changes and are eliminated for the final data set applying the HN minimum limit.

The correction of the HN underestimation caused by settling of the snowpack during snowfall leads to an average reduction

5   of mean ρ_{HN} of 10.2 kg m^{-3} with a standard deviation (σ) of 2.6 kg m^{-3} (Table 2). This corresponds to 13.5 % with a σ of 3.7 %. The compaction correction causes noticeably less change in ρ_{HN} at Weissfluhjoch in period 1 (5 % reduction of mean ρ_{HN}) than at the other time periods and stations. The next closest is Kühroint, also in period 1, with a reduction in ρ_{HN} of 7 %. Unless otherwise stated in the text, ρ_{HN} always refers to the corrected densities hereafter. Based on a 15 year data set of Weissfluhjoch (WSL Institute for Snow and Avalanche Research SLF, doi:10.16904/1.) from 1 September 1999 to 31

10   December 2015, the contribution of settling relative to HN was calculated using the multi-layer SNOWPACK model (e.g. Lehning et al., 2002) and the approach from Anderson (1976) to compare the results of this study to a more physically based estimate. Results are presented in Fig. 3. While a median relative contribution of settling to HN by 19 % was calculated with SNOWPACK, the approach of Anderson (1976) resulted in lower values of 5 % in median and 9 % in mean. Thus, the settling considered for the presented data can be assumed to be lower estimation. However, higher contributions of settling

15   would result in lower ρ_{HN} with increased HN assuming a fixed HNW.

Figure 4 shows the distribution of ρ_{HN} values obtained from the filtered data at Kühroint station as a representative for all stations and periods (Fig. S10 to S17 in the supplement). In general, the ρ_{HN} show high variability at all stations. Nevertheless, ρ_{HN} values are within a reasonable range of less than 200 kg m^{-3}. The histograms of ρ_{HN} show one-tailed distributions towards higher ρ_{HN}. Median ρ_{HN} of the different stations and for different periods range between 66 and 86

20   kg m^{-3} for uncorrected values and between 54 and 83 kg m^{-3} for ρ_{HN} corrected for settling (Table 2).

3.2 Station dependent differences

The distributions of ρ_{HN}, T_w and u during all filtered snowfall data are presented in Fig. 5 and 6 and in Table 2. The lowest T_w and highest wind speeds were observed during snowfall at Weissfluhjoch station. However, the range and distribution of

25   T_w at Weissfluhjoch station result in higher median T_w during snowfall compared to T_w at Wattener Lizum station. With respect to wind speeds, Wattener Lizum is second. Lowest wind speeds at Kühtai station occur together with lowest ρ_{HN}. Weissfluhjoch station has the highest median ρ_{HN} by a large margin with 83 kg m^{-3} in period 1 compared to, respectively, 67, 61 and 66 kg m^{-3} at Kühroint, Kühtai and Wattener Lizum station.

Wind influence may be the reason for higher ρ_{HN} at Weissfluhjoch station. Snow grains are fragmented by snow drift (e.g.

30   Sato et al., 2008), and thus more packed into the layer of new snow during windy conditions even over the course of only one hour. The Kühtai station shows lowest ρ_{HN} and the difference of mean ρ_{HN} is 17 kg m^{-3} between Weissfluhjoch and

Kühtai station for period 1. Median ρ_{HN} and median T_w of the different periods show a relationship between the periods at Kühtai station, with higher ρ_{HN} for higher T_w (Fig. 6, Table 2).

The overall mean hourly ρ_{HN} of all stations and time periods is 68 kg m^{-3} with a standard deviation of 9 kg m^{-3}. In general, this is considerably lower than new snow densities from daily measurements (e.g. Roebber et al., 2003; Egli et al., 2009; Teutsch, 2009). Meister (1985) measured ρ_{HN} lower than 100 kg m^{-3} on a daily basis analysing data with a HN of more than 0.1 m. In contrast, the presented ρ_{HN} are closer to the time of the snowfall event, and density changes over several hours due to e.g. energy exchanges and wind drift at the uppermost snow layer can be excluded. On the basis of ρ_{HN} in-situ measurements in hourly resolution Lehning et al. (2002) emphasized that at sub-daily time intervals lower densities in comparison to daily new snow densities have to be applied. Comparatively low ρ_{HN} values close to 50 kg m^{-3} were also presented by Ishizaka et al. (2016), with an average ρ_{HN} of 52 kg m^{-3} for aggregated snowflakes and 55 kg m^{-3} for small hydrometeors. They further found a mean ρ_{HN} of 72 kg m^{-3} for a second group of smaller crystals and 99.4 kg m^{-3} for graupel type hydrometeors.

The observed inter-station variability shows the importance of differing ρ_{HN} between more windy mountain stations and less windy stations in the valleys.

3.3 Density parametrisations

A simple linear regression analysis showed that the short term variability of ρ_{HN} cannot be explained with corresponding changes in T_w or u (Table 3, Fig. 7 and S18 to S26). An increase of ρ_{HN} with increasing T_w can be identified in the figures, and the slopes of the least squares regressions show an increase of ρ_{HN} with an increase of wet bulb temperature for all stations (Table 3). However, no consistent relationship between ρ_{HN} and u could be found neither for single stations nor for different periods at one station. The binned analysis based on T_w showed a considerable r^2 of more than 0.5 on a 0.01 significance level at Kühroint and Kühtai station, with intercepts of 70 to 80 kg m^{-3} and gradients of about 3 to 4 kg m^{-3} per 1°C.

Although the regressions generally show the expected trends, it must be noted that the variability of ρ_{HN} remains unexplained. This could partly be attributed to the measurement uncertainties. However, the variability caused by measurement uncertainties is assumed to be equalized considering mean and median of ρ_{HN} values only for total time periods. Relationships between ρ_{HN} and T_w were recognized for distinct periods and stations only, but with a similar coefficients of determination in comparison to the results of e.g. Judson and Doesken (2000), Wetzel et al. (2004) or Wright et al. (2016).

Testing multiple regressions using additional meteorological parameters didn't increase the statistical significance. Instead a comparison to existing parameterizations of ρ_{HN} was performed for all stations and periods.

Considering the various parameterizations, which use meteorological parameters to approximate new snow density (Eq. 3 to 9), it is evident that the observed variability of ρ_{HN} is not correlated to the variability of parameterized new snow densities (Table 4). Most of the seven parametrizations overestimate the median of the observed ρ_{HN} values (Fig. 3, 7 and 8, Table 4). However, some parameterizations produce considerably better results than others for median ρ_{HN} values. The parameterizations of LaChapelle (1962), Diamond and Lowry (1954) and Vionnet et al., (2012) consistently overestimate ρ_{HN}. The parameterization of Hedstrom and Pomeroy (1998) overestimates ρ_{HN} at Kühroint, Kühtai and Wattener Lizum station (Fig. 7 and 8), but converges with the median ρ_{HN} at Weissfluhjoch station for period 1 (Fig. 7, Table 4). In general, the ρ_{HN} simulated using the parameterization of Jordan et al. (1999) are closer to calculated ρ_{HN}, but median ρ_{HN} are underestimated for Weissfluhjoch station. Median ρ_{HN} and the range of ρ_{HN} at Weissfluhjoch are well simulated using the parameterization of Schmucki et al. (2014), but it overestimates median ρ_{HN} of Kühroint, Kühtai and Wattener Lizum station (Fig. 3 and 7, Table 4). However, this parameterization was fitted to original density data from Weissfluhjoch.

The lowest root mean squared error (R) was achieved for Weissfluhjoch station with the parameterization of Diamond and Lowry (1954). The parameterizations of Lehning et al. (2002) and Jordan et al. (1999) result in lowest R (Table 4) compared to ρ_{HN} at Kühroint, Kühtai and Wattener Lizum station, with slightly lower density values using the parameterization of Lehning et al. (2002) fitting best to the low median ρ_{HN} values of the Kühtai station.

Thus, the parameterization of Lehning et al. (2002) appears to be the first choice regarding the calculation of hourly new snow densities for high elevations and inner alpine regions. This parameterization requires multiple input parameters. Where such data is not available, the parameterization of Jordan et al. (1999), requiring temperature and wind data only, might be a good alternative. Even though, correlations are low in general, some of the highest Pearson correlation values (r, Table 4) were achieved by applying the simpler, linear equations by Diamond and Lowry (1954), LaChapelle (1962) and Vionnet et al. (2012). In addition to the regressions presented in Table 3, this shows again the identifiable relation between snow density and temperature.

Mair et al. (2015) evaluated some of the parameterizations also considered in this study. Using a distinctly larger time window for smoothing their HS data (5-hour-average), they calculated median ρ_{HN} between 75 and 100 kg m^{-3} using the parameterizations of Jordan et al. (1999) and Hedstrom and Pomeroy (1998), which is close to the results presented in this study. They also found that using the parameterization of LaChapelle (1962) results in mean ρ_{HN} higher than 100 kg m^{-3}. In general they concluded that using a constant ρ_{HN} of 100 kg m^{-3} caused an overestimation of seasonal precipitation by up to 30 %. Conversely, a mean ρ_{HN} of 70 kg m^{-3} will result in better SWE estimations. This is in accordance with the resulting average ρ_{HN} of 68 kg m^{-3} calculated from automated measurements within our study.

4 Conclusion

The aim of this study was to assess the value of automated measurements of snow depth (HS) and snow water equivalent (SWE) to compute new snow density (ρ_{HN}) on an hourly time interval. Complementary data sets of HS and SWE measurements using ultrasonic devices and snow pillows from four mountain stations were used to calculate the height of new snow (HN) and the water equivalent of snowfall (HNW). Subsequently, ρ_{HN} was calculated from HN and HNW considering potential underestimation of HN by settling of the snowpack.

The snow measurements using ultrasonic devices and snow pillows were found to be appropriate for the calculation of station average hourly ρ_{HN} values. However, the observed variability in ρ_{HN} from the automated measurements could not be described with appropriate statistical significance by any of the investigated algorithms. An average ρ_{HN} of 68 kg m^{-3} with a standard deviation of 9 kg m^{-3} was calculated considering all stations and time periods. Average ρ_{HN} for individual stations in a common period ranged from 61 kg m^{-3} to 83 kg m^{-3}, whit higher ρ_{HN} at more windy locations. Thus, wind speed is a crucial parameter for the inter-station variability of $\rho_{HN.}$

Seven existing parameterizations for estimating new snow densities were tested, and most calculations overestimate ρ_{HN} in comparison to the results from the hourly automated measurements. Two of the tested parameterizations were capable of simulating low ρ_{HN} at sheltered inner-alpine stations. This reveals that it has to be carefully considered which parameterization should be used for which application and environment.

Nevertheless, the natural variability of ρ_{HN} is masked using the combination of ultrasonic ranging and snow pillow data for ρ_{HN} calculation, because of the limited accuracy of the sensors and snow depth changes due to settling of the snowpack and wind drift. We conclude that the value of the analysed data is given by the mean and median ρ_{HN} and its variation between different stations and time periods, and the considerably lower ρ_{HN} values in contrast to ρ_{HN} calculated on daily or event-based measurements.

The study shows the potential of collocated measurements of HS and SWE for determining ρ_{HN} automatically. However, recent developments in optical distance sensors and weighing devices increase the accuracy of such snow measurements and hence decrease the uncertainty of subsequent calculations. We therefore recommend the use of high accuracy sensors for the determination of ρ_{HN} on sub daily intervals.

Data availability

A processed set of SNOWPACK input data from Weissfluhjoch station is available at: *WSL Institute for Snow and Avalanche Research SLF (2015): WFJ_MOD: Meteorological and snowpack measurements from Weissfluhjoch, Davos, Switzerland; WSL Institute for Snow and Avalanche Research SLF; doi:10.16904/1.*

5 Detailed information about the Weissfluhjoch data set can be found in WSL Institute for Snow and Avalanche Research SLF (2015) and in Marty and Meister (2012). Data of Kühtai station are published by Krajči et al. (2017) and are available from the Zenodo repository doi:10.5281/zenodo.556110.

Data of Kühroint station are available on request from the Bavarian avalanche service (https://www.lawinenwarndienst-bayern.de/organisation/lawinenwarnzentrale/kontakt.php).

10 Data of Wattener Lizum station are available on request from the Austrian Federal Research and Training Centre for Forests, Natural Hazards and Landscap (BFW, https://bfw.ac.at/rz/bfwcms.web?dok=6057).

Author contribution

Kay Helfricht is the main investigator of this study. Lea Hartl performed snow density analysis within the pluSnow project.
15 Roland Koch performed initial quality control, provision and setup of project database for all station and meta data. Christoph Marty prepared the data of Weissfluhjoch station, contributed fruitful discussions and helped to focus the analysis and the manuscript. Marc Olefs contributed significantly to analysis and discussions as the main project partner within the framework of the pluSnow project.

20 **Competing Interests**

The authors declare that they have no conflict of interest.

Acknowledgements

The pluSnow project is financed by the Gottfried and Vera Weiss Science Foundation (WWW). The project funding is
25 managed in trust by the Austrian Science Fund (FWF): P 28099-N34. Project duration 10/2015 - 09/2018. The authors want to thank the colleagues of the Tiroler Wasserkraft AG (TIWAG), of the Federal Research and Training Centre for Forests

(BFW) and of the Bavarian avalanche service for data provision. In particular we are grateful for the close collaboration by Johannes Schöber (TIWAG) and Reinhard Fromm (BFW). We also want to thank Michael Lehning, Charles Fierz and the two reviewers for their helpful comments and fruitful discussion of the results.

References

5 Alcott, T. I., and Steenburgh, W. J. : Snow-to-Liquid Ratio Variability and Prediction at a High-Elevation Site in Utah's Wasatch Mountains, Wea. Forecasting, 25, 323–337, doi: 10.1175/2009WAF2222311.1, 2010.

Anderson, E. A.: A point energy and mass balance model of a snow cover. NOAA Tech. Rep. NWS-19, 150 pp, 1976.

Buisán, S. T., Earle, M. E., Collado, J. L., Kochendorfer, J., Alastrué, J., Wolff, M., Smith, C. D., and López-Moreno, J. I.: Assessment of snowfall accumulation underestimation by tipping bucket gauges in the Spanish operational network,

10   Atmos. Meas. Tech., 10, 1079-1091, doi:10.5194/amt-10-1079-2017, 2017.

Diamond, M., and Lowry, W. P.: Correlation of density of new snow with 700-millibar temperature. J. Meteor., 11, 512–513, 1954.

Egli, L., Jonas, T., and Meister, R.: Comparison of different automatic methods for estimating snow water equivalent, Cold Regions Sci. Technol., 57, 107–115, doi: 10.1016/j.coldregions.2009.02.008, 2009.

15 Fierz, C., Armstrong, R. L., Durand, Y., Etchevers, P., Greene, E., McClung, D. M., Nishimura, K., Satyawali, P. K., and Sokratov S. A.: The International Classification for Seasonal Snow on the Ground, IHP- VII Technical Documents in Hydrology N°83, IACS Contribution N°1, UNESCO- IHP, Paris, 2009.

Gold, L. W. and Power, B. A.: Correlation of snow crystal type with estimated temperature of formation, J. Meteor., 9, 447, 1952.

20 Goodison, B. E., Wilson, B., We, K., and Metcalfe, J. R.: An inexpensive remote snow depth gauge: an assessment. The 52th Western Snow Conference. Sun Valley, Idaho, April 17–19, 1984.

Goodison, B. E., Louie, P. Y. T., and Yang, D.: WMO solid precipitation measurement intercomparison. Final Report; World Meteorological Organization, No. 872, 212 pp., 1998.

Gubler, H.: An Inexpensive Remote Snow-Depth Gauge based on Ultrasonic Wave Reflection from the Snow Surface.

25   Journal of Glaciology, 27(95), 157-163, doi:10.3189/S002214300001131X, 1981.

Hedstrom, N. R., and Pomeroy, J. W.: Measurements and modeling of snow interception in the boreal forest, Hydrol. Processes, 12, 1611–1625, doi:10.1002/(SICI)1099-1085(199808/09)12:10/11<1611::AID-HYP684>3.0.CO;2-4, 1998.

Heilig, A., Schneebeli, M., and Eisen, O.: Upward-looking ground-penetrating radar for monitoring snowpack stratigraphy,

30   Cold Reg. Sci. Technol., 59, 152–162, doi: 10.1016/j.coldregions.2009.07.008, 2009.

Helfricht, K., Koch, R., Hartl, L. and Olefs, M.: Potential and Challenges of an extensive operational use of high accuracy optical snow depth sensors to minimize solid precipitation undercatch. Proceedings of the 16th International Snow Science Workshop ISSW, Breckenridge, Colorado, 3.-7.10.2016, 631-635, 2016.

Ishizaka, M., Motoyoshi, H., Yamaguchi, S., Nakai, S., Shiina, T., and Muramoto, K.-I.: Relationships between snowfall density and solid hydrometeors, based on measured size and fall speed, for snowpack modeling applications, The Cryosphere, 10, 2831-2845, doi:10.5194/tc-10-2831-2016, 2016.

Johnson, J. B. and Schaefer, G. L.: The influence of thermal, hydrologic, and snow deformation mechanisms on snow water equivalent pressure sensor accuracy. Hydrol. Process., 16: 3529–3542. doi:10.1002/hyp.1236, 2002.

Jordan, R. E., Andreasand, E. L. and Makshtas, A. P.: Heat budget of snow-covered sea ice at North Pole , J. Geophys. Res., 104(C4), 7785–7806, doi: 10.1029/1999JC900011, 1999.

Judson, A.: The weather and climate of a high mountain pass in the Colorado Rockies, Research Paper RM-16, USDA Forest Service, Fort Collins, CO, 28 pp., 1965.

Judson, A., and Doesken, N.: Density of Freshly Fallen Snow in the Central Rocky Mountains, Bull. Amer. Meteor. Soc., 81, 1577–1587, doi: 10.1175/1520-0477(2000)081<1577:DOFFSI>2.3.CO;2, 2000.

Koch, F., Prasch, M., Schmid, L., Schweizer, J., and Mauser, W.: Measuring Snow Liquid Water Content with Low-Cost GPS Receivers, Sensors, 14(11), 20975-20999, doi: 10.3390/s141120975, 2014.

Krajči, P., Kirnbauer, R., Parajka, J., Schöber, J. and Blöschl G.: The Kühtai data set: 25 years of lysimetric, snow pillow, and meteorological measurements, Water Resour. Res., 53, 5158–5165, doi:10.1002/2017WR020445, 2017.

LaChapelle, E. R.: The density distribution of new snow, USDA Forest Service, Alta Avalanche Study Center, Project F, Progress Rep. 2, Salt Lake City, UT, 13 pp., 1962.

Lehning, M., Bartelt, P., Brown, B., and Fierz, C.: A physical SNOWPACK model for the Swiss avalanche warning. Part III: meteorological forcing, thin layer formation and evaluation, Cold Reg. Sci. Technol., 35(3), 169–184, doi: 10.1016/S0165-232X(02)00072-1, 2002.

Lundberg, A., Granlund, N., and Gustafsson, D.: Towards automated "Ground truth" snow measurements: a review of operational and new measurement methods for Sweden, Norway, and Finland, Hydrol. Process., 24, 1955-1970, doi: 10.1002/hyp.7658, 2010.

Mair, M., and Baumgartner, D. J.: Operational experience with automatic snow depth sensors – ultrasonic and laser principle. In TECO, ed. WMO. Helsinki, Finland: WMO, 2010.

Mair, E., Leitinger, G., Della Chiesa, S., Niedrist, G., Tappeiner, U., and Bertoldi, G.: A simple method to combine snow height and meteorological observations to estimate winter precipitation at sub-daily resolution, Hydrological Sciences Journal, doi: 10.1080/02626667.2015.1081203, 2015.

Marty, C. and Meister, R.: Long-term snow and weather observations at Weissfluhjoch and its relation to other high-altitude observatories in the Alps. Theor. Appl. Climatol., 110, 573-583, https://doi.org/10.1007/s00704-012-0584-3, 2012

McCreight, J. L., Small, E. E., and Larson, K. M.: Snow depth, density, and SWE estimates derived from GPS reflection data: Validation in the western U. S., Water Resour. Res., 50, 6892–6909, doi: 10.1002/2014WR015561, 2014.

5   Meister, R.: Density of New Snow and its Dependence of Air Temperature and Wind, Workshop on the Correction of Precipitation Measurements, 1 - 3 April 1985, Zurich, Volume: B, Sevruk (ed.) Correction of Precipitation Measurements. Zürcher Geographische Schriften No. 23, 1985.

McKay, G.A., and Gray, D.M.: The distribution of snow cover. In Handbook of Snow. Principles, Processes, Management and Use, D.M. Gray and D.H. LMale (Eds.). Pergamon Press, Toronto, 1981.

10   Morin, S., Lejeune, Y., Lesaffre, B., Panel, J.-M., Poncet, D., David, P., and Sudul, M.: An 18-yr long (1993–2011) snow and meteorological dataset from a mid-altitude mountain site (Col de Porte, France, 1325 m alt.) for driving and evaluating snowpack models, Earth Syst. Sci. Data, 4, 13-21, https://doi.org/10.5194/essd-4-13-2012, 2012.

Nakaya, U.: The formation of ice crystals, Compendium Meteor. Boston, Amer. Meteor. Soc., 207-220, 1951.

Nitu, R., et al.: WMO Intercomparison of instruments and methods for the measurement of precipitiation and snow on the

15   ground. In 9th International Workshop on Precipitation in Urban Areas, 6. St. Moritz, Switzerland. 2012

Olefs, M., Fischer, A., and Lang, J.: Boundary conditions for artificial snow production in the Austrian Alps. J. Appl. Meteorol. Climatol., 49(6): 1096-113, doi: http://dx.doi.org/10.1175/2010JAMC2251.1, 2010.

Olefs, M., Schöner, W., Suklitsch, M., Wittmann, C., Niedermoser, B., Neururer, A., and Wurzer. A.: SNOWGRID – A New Operational Snow Cover Model in Austria. In International Snow Science Workshop. Grenoble – Chamonix Mont-

20   Blanc, 2013.

Pahaut, E.: La m´etamorphose des cristaux de neige (Snow crystal metamorphosis), 96, Monographies de la M´et´eorologie Nationale, M´et´eo France, 1976.

Power, B. A., Summers, P. W., and D'Avignon, J.: Snow crystal forms and riming effect as related to snowfall density and general storm conditions, J. Atmos. Sci., 21, 300–305, doi:10.1175/1520-

25   0469(1964)021<0300:SCFARE>2.0.CO;2, 1964.

Roebber, P. J., Bruening, S. L., Schultz, D. M., and Cortinas, J.V.: Improving Snowfall Forecasting by Diagnosing Snow Density, Wea. Forecasting, 18, 264–287, doi: 10.1175/1520-0434(2003)018<0264:ISFBDS>2.0.CO;2., 2003.

Sato, T., Kosugi, K., Mochizuki, S., and Nemoto, M.: Wind speed dependences of fracture and accumulation of snowflakes on snow surface, Cold Reg. Sci. Technol., 51, 229–239, doi: 10.1016/j.coldregions.2007.05.004, 2008.

30   Schattan, P., Baroni, G., Oswald, S.E., Schöber, J., Fey, C., Kormann, C., Huttenlau, M. and Achleitner, S.: Continuous Monitoring of Snowpack Dynamics in Alpine Terrain by Above-Ground Neutron Sensing. Water Resources Research, 53, 1-20, 2017.

Schmid, L., Koch, F., Heilig, A., Prasch, M., Eisen, O., Mauser, W., and Schweizer, J.: A novel sensor combination (upGPR-GPS) to continuously and nondestructively derive snow cover properties, Geophys. Res. Lett., 42, 3397–3405. doi: 10.1002/2015GL063732, 2015.

Smith, C. D., Kontu, A., Laffin, R., and Pomeroy, J. W.: An assessment of two automated snow water equivalent instruments during the WMO Solid Precipitation Intercomparison Experiment, The Cryosphere, 11, 101-116, doi:10.5194/tc-11-101-2017, 2017.

Schmid, L., Heilig, A., Mitterer, C., Schweizer, J., Maurer, H., Okorn, R., & Eisen, O.: Continuous snowpack monitoring using upward-looking ground-penetrating radar technology. *Journal of Glaciology, 60*(221), 509-525. doi:10.3189/2014JoG13J084, 2014

Schmidt, R. A and Gluns, D. R.: Snowfall interception on branches of three conifer species, Can. J. For. Res., 21, 1262-1269, doi: 10.1139/x91-176, 1991.

Schmucki, E., Marty, C., Fierz, c. and Lehning, M.: Evaluation of modelled snow depth and snow water equivalent at three contrasting sites in Switzerland using SNOWPACK simulations driven by different meteorological data input, Cold Reg. Sci. Technol., 99, 27-37, doi: 10.1016/j.coldregions.2013.12.004, 2014.

Schöber, J., Achleitner, S., Bellinger, J., Kirnbauer, R, and Schöberl, F.: Analysis and modelling of snow bulk density in the Tyrolean Alps. Hydrology Research, 47 (2) 419-441; DOI: 10.2166/nh.2015.132, 2016.

Serreze, M.C., Clark, M.P., Armstrong, R.L., McGinnis, D.A. and Pulwarty, R.S.: Characteristics of the western United States snowpack from snowpack telemetry (SNOTEL) data, Water Resources Research, 35(7), 2145-2160, doi: 10.1029/1999WR900090, 1999.

Simeral, D. B.: New snow density across an elevation gradient in the Park Range of northwestern Colorado, M.A. thesis, Department of Geography, Planning and Recreation, Northern Arizona University, 101 pp., 2005.

Sonntag, D.: Important new values of the physical constants of 1986, vapour pressure formulations based on the ITS-90, and psychrometer formulae. Z. Meteorol., 70, 340-344, 1990.

Steinkogler, W.: Systematic Assessment of New Snow Settlement in SNOWPACK, M.A. thesis, University of Innsbruck, Institute of Meteorology and Geophysics, 96 pp., 2009.

Teutsch, C.: Neuschneedichtenanalyse in den Ostalpen. M.A. thesis, Institute of Meteorology and Geophysics, Innsbruck, Austria, University of Innsbruck, 2009.

US Army Corps of Engineers: Snow Hydrology: Summary Report of the Snow Investigations, North Pacific Division, Portland, Oregon. 437 pp., 1956.

Valt, M., Chiambretti, I., and Dellavedova, P.: Fresh snow density on the Italian Alps, Geophysical Research Abstracts, 16, EGU2014-9715, 2014.

Vionnet, V., Brun, E., Morin, S., Boone, A., Faroux, S., Le Moigne, P., Martin, E., and Willemet, J.-M.: The detailed snowpack scheme Crocus and its implementation in SURFEX v7.2, Geosci. Model Dev., 5, 773-791, doi: 10.5194/gmd-5-773-2012, 2012.

Wetzel, M., Meyers, M., Borys, R., McAnelly, R., Cotton, W., Rossi, A., Frisbie, P., Nadler, D., Lowenthal, D., Cohn, S. and Brown, W.: Mesoscale Snowfall Prediction and Verification in Mountainous Terrain. Wea. Forecasting, 19, 806–828, https://doi.org/10.1175/1520-0434(2004)019<0806:MSPAVI>2.0.CO;2, 2004.

Wright, P. J., Comey, B., McCollister, C., and Rheam, M.: Estimation of the new snow density using 42 seasons of meteorological data from Jackson Hole Mountain Resort, Wyoming, Proceedings, International Snow Science Workshop, Breckenridge, Colorado, 1180-1185, 2016.

WSL Institute for Snow and Avalanche Research SLF: WFJ_MOD: Meteorological and snowpack measurements from Weissfluhjoch, Davos, Switzerland, WSL Institute for Snow and Avalanche Research SLF, doi: 10.16904/1, 2015.
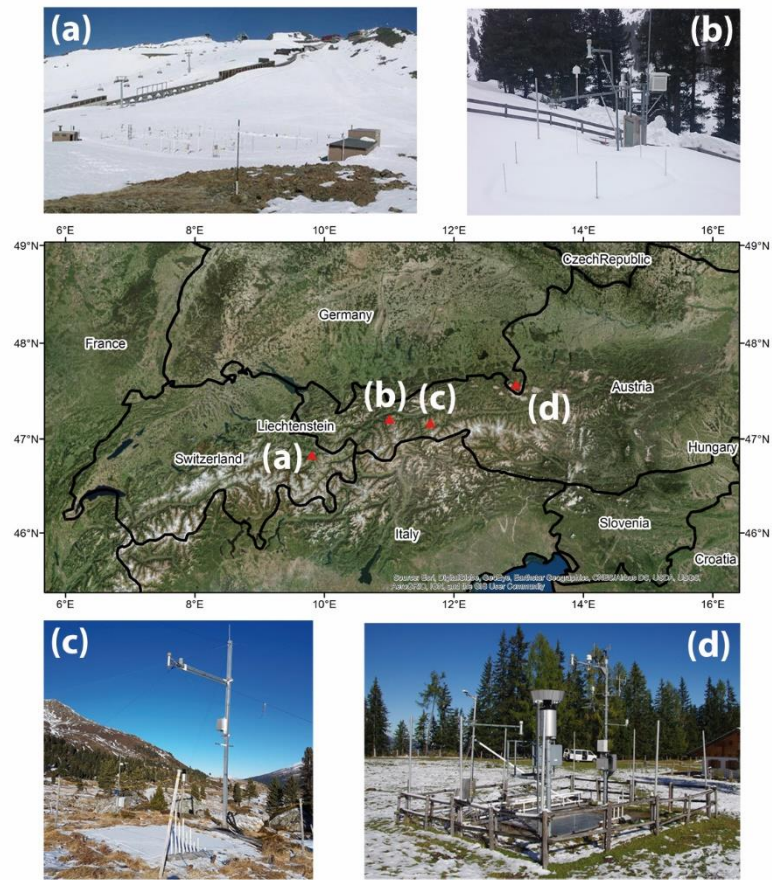
Figure 1: Map of the station locations. Pictures are given for (a) Weissfluhjoch station, (b) Kühtai station, (c) Wattener Lizum station and (d) Kühroint station.
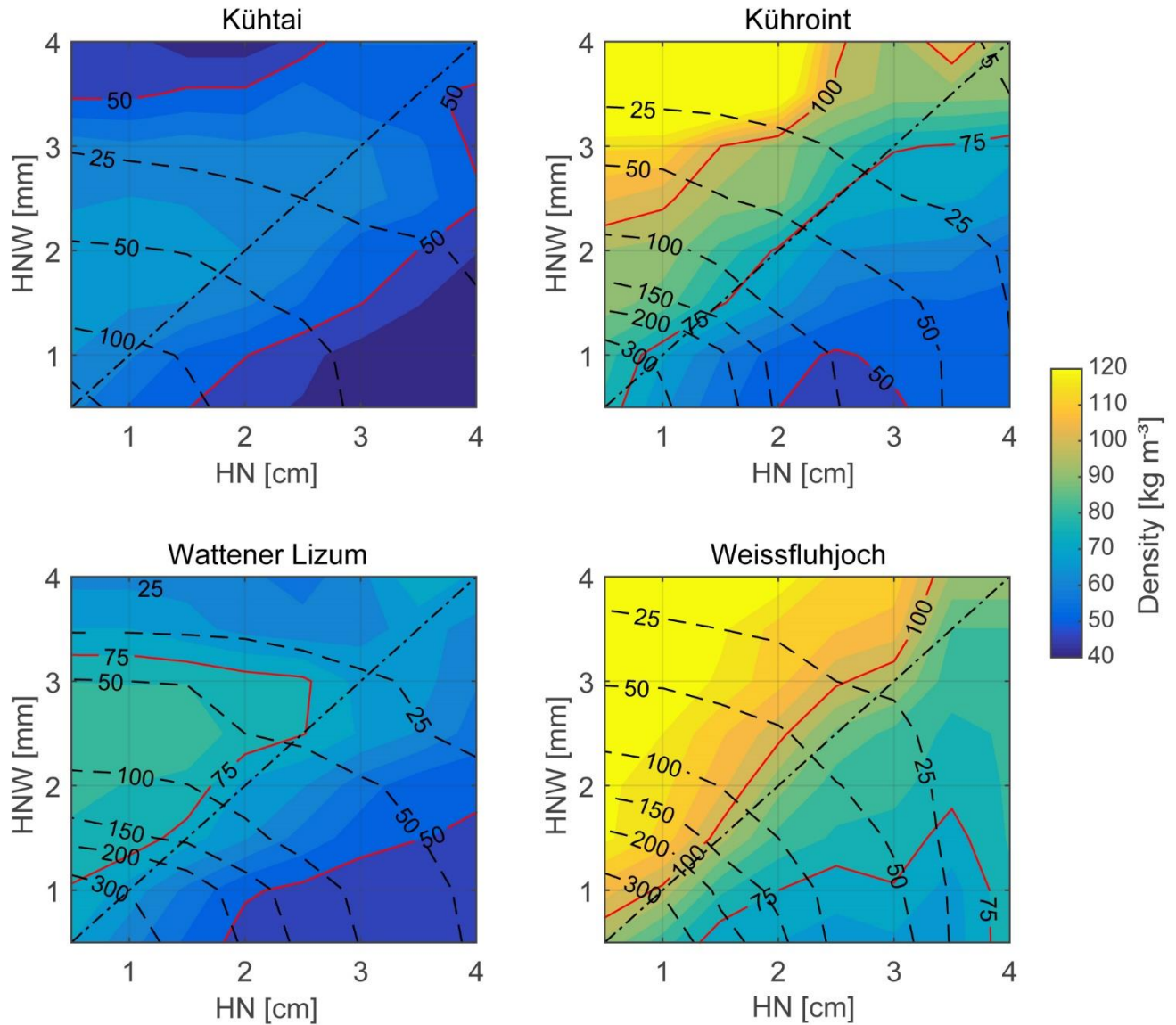
Figure 2: Median new snow densities (colour scale) calculated using all data exceeding different minimum limits of the height of new snow (HN) and the water equivalent of snowfall (HNW) for the period 1 (1 Oct 2013 - 20 May 2015). Note that multiples of 25 kg m^{-3} are highlighted with red contour lines. The labelled black dashed lines give the count of the hourly data remaining after filtering. The straight dot-dashed lines show results for equal minimum limits of HN [cm] and HNW [mm].
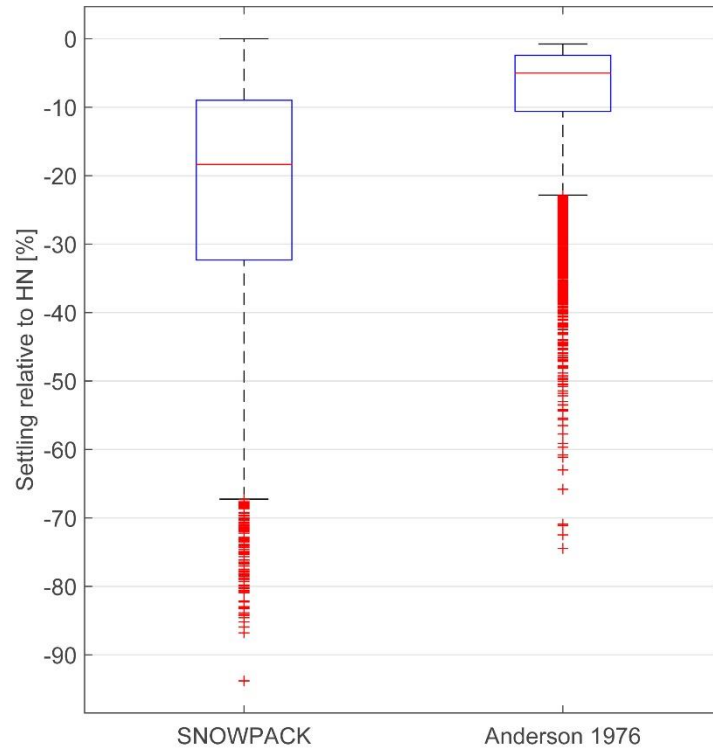
Figure 3: Boxplots (Median, 25% and 75% percentiles, 1.5 x interquartile ranges, outliers) of settling relative to hourly new snow heights (HN) modelled with SNOWPACK and using the approach presented by Anderson (1976).
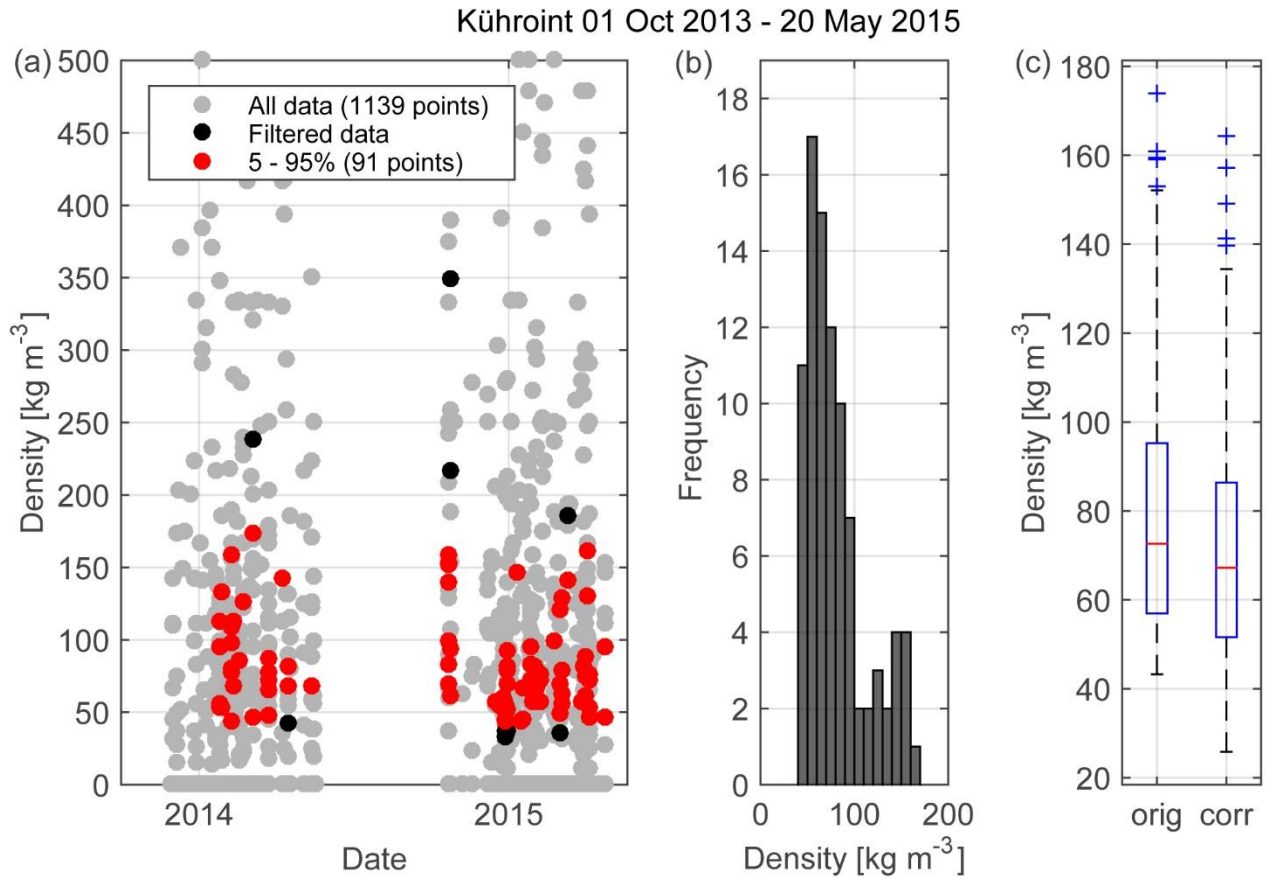
Figure 4: Distribution of calculated new snow densities at Kühroint station for the period 1 (1 Oct 2013 - 20 May 2015). (a) All data with precipitation signal and positive HS change, all data filtered with HN > 2 cm, HNW > 1.5 mm, Tw < 0°C and u < 5 ms^{-1}), and filtered data reduced by cutting off at 5 % and 95 % percentiles. (b) Histogram of all filtered densities. (c) The boxplot showing median, 25 % and 75 % interquartile range of uncorrected densities and densities corrected for settling of the snowpack. Note that similar figures are available in the supplement (Fig. S10 – S17) for all stations and all time periods considered in this study.
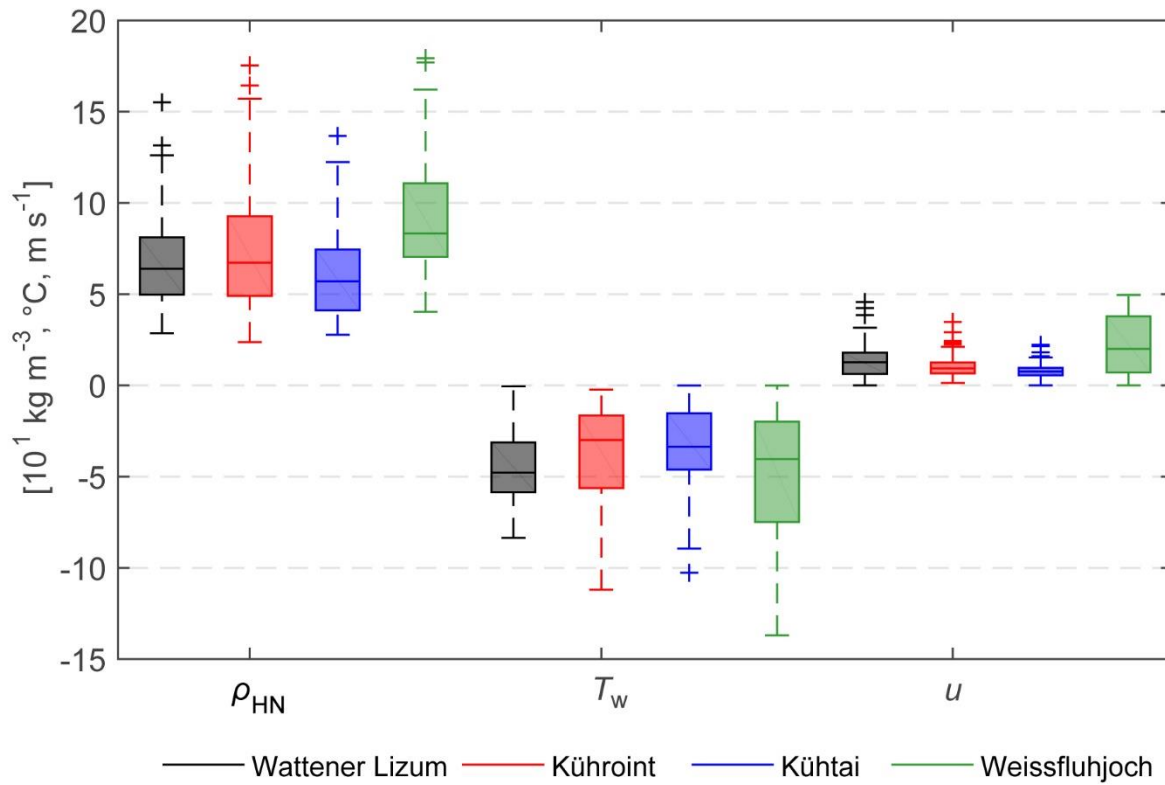
Figure 5: Boxplot (Median, 25% and 75% percentiles, 1.5 x interquartile ranges, outliers) of calculated new snow densities (ρ_{HN}) based on observations, wet bulb temperature (T_w) and wind speed (u) for filtered snowfall events (Table 2) at all four stations within period 1 (1 Oct 2013 - 20 May 2015).
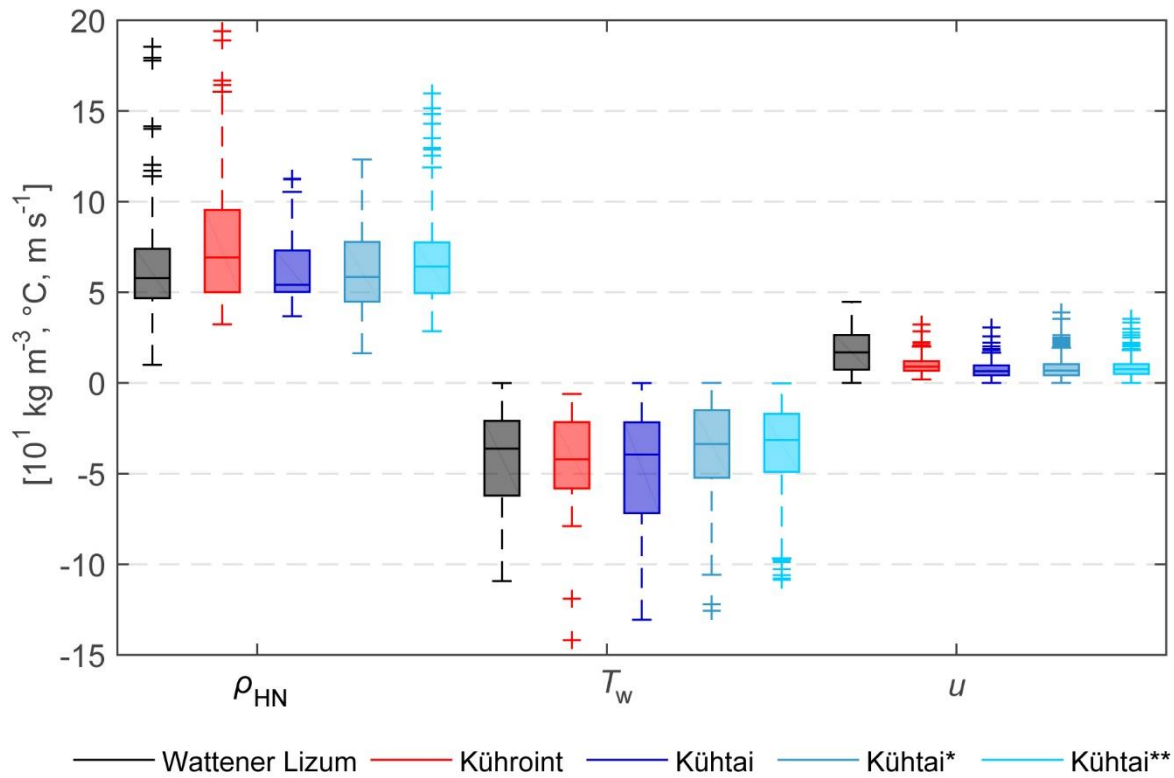
Figure 6: Boxplots (Median, 25% and 75% percentiles, 1.5 x interquartile ranges, outliers) of calculated new snow densities (ρ_{HN}) based on observations, wet bulb temperature (T_w) and wind speed (u) for filtered snowfall events (Table 2) at three stations within period 2 (1 Oct 2011 - 01 Oct 2013) and at Kühtai station within period 3 (index *, 01 Oct 1999 - 30 Sep 2011) and period 4 (index
5   ****, 27 Feb 1987 – 30 Sep 1999) .**

Figure 7: Boxplots (Median, 25% and 75% percentiles, 1.5 x interquartile ranges, outliers) of calculated new snow densities (ρ_{HN}) based on observations and densities calculated using parameterizations developed in previous studies (Eq. (3) – (9)) at all four stations within period 1 (1 Oct 2013 - 20 May 2015).
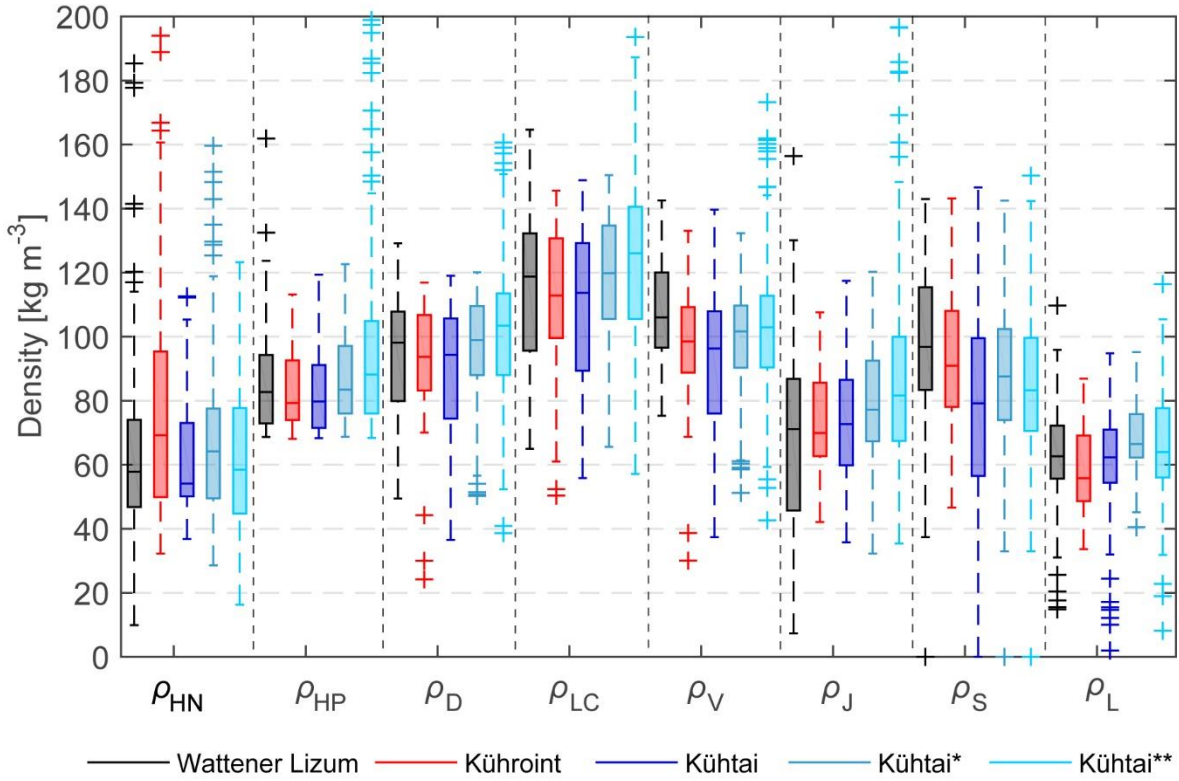
Figure 8: Boxplots (Median, 25% and 75% percentiles, 1.5 x interquartile ranges, outliers) of calculated new snow densities (ρ_{HN}) based on observations and densities calculated using parameterizations developed in previous studies (Eq. (3) – (9)) at three stations within period 2 (1 Oct 2011 - 01 Oct 2013) and at Kühtai station within period 3 (index *, 01 Oct 1999 - 30 Sep 2011) and period 4 (index **, 27 Feb 1987 – 30 Sep 1999).

Table 1: Coordinates and data availability of the four snow stations are given. The instrumentations for measuring snow depth (HS), snow water equivalent (SWE), temperature (*T*), relative humidity (*rH*), precipitation (*P*), wind speed (*u*) and global radiation (*r*) are listed.

	Station Abbreviation	Kühroint KRO	Kühtai KTA	Wattener Lizum WAL	Weissfluhjoch WFJ
Location	East	12°57'35.5"	11°00'21.6"	11°38'18.6"	9°48'35.7"
	North	47°34'12.4"	47°12'25.6"	47°10'05.5"	46°49'46.4"
	z (m a.s.l.)	1420	1970	1994	2540
Data		01 Jan 2011 - 02 Dec 2015	27 Feb 1987 - 20 May 2015	01 Oct 2010 – 30 Dec 2016	01 Oct 2013 - 29 Sep 2015
Instruments	HS	Sommer USH 8	Sommer USH 8	Sommer USH 8	Campbell Scientific SR50A
	SWE	Sommer Snow Scale SSG	OTT Thalimedes Shaft Encoder, Endress+Hauser Deltapilot M	Sommer Snowpillow	Sommer Snowpillow
	T	Rotronic MP408	Kroneis NTC	Vaisala HMP45C	Rotronic Hydroclip S3
	rH	Rotronic MP408	Pernix hair hygrometer	Vaisala HMP45C	Rotronic Hydroclip S3
	P	Sommer NIWA/Med-K505	Ott Pluvio since 2001, custom built tipping bucket before	Sommer NIWA/Med-K505	Lambrecht Pluvio 1518 H3
	u	Young 05103	Kroneis cup anemometer + vane	YOUNG Wind Monitor	Young 05103
	r	Schenk 8101	Schenk 8101	Kipp&Zonen CM21	Kipp&Zonen CM21
Comments			data gap winter 2012/13, wind regionalized from 1999	Meteorological measurements at 2041 m a.s.l.	

Table 2: Time periods analysed in this study with mean and the median of hourly values for the height of new snow (HN), wet bulb temperature (T_w), wind speed (u), calculated densities from observed values (ρ) and calculated densities corrected for settling of the snowpack (ρ_{HN}). The results are valid for the filtered data values (n_{th}) with HN > 2 cm, HNW > 1.5 mm, $T_w < 0°$ C and $u < 5$ ms^{-1} as a subset of all data consisting precipitation signal and positive HS change (n_P).

Station	#	Period	count data n_p	n_{th}	HN [cm] mean	median	T_w [°C] mean	median	u [m s^{-1}] mean	median	ρ [kg m^{-3}] mean	median	ρ_{HN} [kg m^{-3}] mean	median
KRO	1	1 Oct 2013 - 20 May 2015	1139	91	3.2	3.1	-3.9	-3.0	1.1	0.9	82	73	73	67
	2	1 Oct 2011 - 30 Sep 2013	1576	118	3.4	3.1	-4.2	-4.2	1.0	0.9	87	77	74	69
KTA	1	1 Oct 2013 - 20 May 2015	579	53	3.8	3.3	-3.4	-3.4	0.8	0.8	70	69	61	61
	2	1 Oct 2011 - 30 Sep 2013	506	36	3.3	2.8	-4.8	-4.0	0.8	0.7	75	66	60	54
	3	1 Oct 1999 - 30 Sep 2011	5293	252	3.5	3.2	-3.5	-3.2	0.8	0.8	74	74	64	64
	4	27 Feb 1987 - 30 Sep 1999	7958	387	3.7	3.3	-3.6	-3.4	0.8	0.7	74	75	61	59
WAL	1	1 Oct 2013 - 20 May 2015	1248	111	3.6	3.4	-4.3	-4.8	1.3	1.3	76	72	68	66
	2	1 Oct 2011 - 30 Sep 2013	1588	126	3.9	3.5	-4.3	-3.6	1.7	1.7	71	69	62	58
WFJ	1	1 Oct 2013 - 20 May 2015	1619	100	3.0	2.7	-4.9	-4.0	2.2	2.0	95	86	91	83

Table 3: Results of a single linear regression between the corrected densities (ρ_{HN}) as dependent variable and wet bulb temperature (T_w) as well as wind speed (u) as explanatory variables for the class median values based on all filtered data points binned into 0.5° K classes and classes of 0.5 ms^{-1}, respectively. The corresponding coefficient of determination (r²) and the p – value are presented.

Station	Period #	T_w				u			
		Intercept	$\delta\rho/\delta T_w$	r^2	p	Intercept	$\delta\rho/\delta u$	r^2	p
KRO	1	82.07	4.00	0.65	0.00	45.12	19.10	0.35	0.16
	2	76.54	0.99	0.11	0.35	64.84	1.29	0.00	0.90
KTA	1	66.37	1.84	0.12	0.44	72.59	-14.44	0.41	0.36
	2	55.15	-0.37	0.02	0.75	54.25	3.37	0.53	0.17
	3	68.18	1.51	0.56	0.01	64.81	-3.82	0.39	0.10
	4	72.41	3.75	0.82	0.00	49.31	9.41	0.30	0.26
WAL	1	78.84	2.88	0.47	0.06	65.28	1.32	0.02	0.71
	2	64.58	0.97	0.17	0.21	59.43	1.50	0.05	0.57
WFJ	1	92.68	0.71	0.04	0.53	92.88	-2.91	0.18	0.23

Table 4: Comparison of corrected density values (ρ_{HN}, [kg m^{-3}]) and parameterizations applying the Eq. (3) to (9) presented in section 2. Median values (m, [kg m^{-3}]) are shown together with the Pearson correlation coefficient (r) and the root mean squared error (R, [kg m^{-3}]) between the respective calculations and ρ_{HN}. Best values of the performance measures are highlighted for each station and time period using underlined bold numbers.

Stat	Period #	ρ_{HN} m	ρ_{HP} m	r	R	ρ_D m	r	R	ρ_{LC} m	r	R	ρ_V m	r	R	ρ_J m	r	R	ρ_S m	r	R	ρ_L m	r	R
KRO	1	67	85	0.28	14.4	100	0.45	23.3	121	0.44	44.4	101	**0.47**	25.3	75	0.29	**0.5**	92	0.36	18.9	60	0.40	15.8
	2	69	79	0.18	8.7	94	0.18	18.8	113	0.19	38.8	99	0.13	25.7	70	**0.20**	**1.0**	91	0.10	19.8	56	**0.20**	14.5
KTA	1	61	82	0.35	28.7	98	**0.38**	40.1	118	**0.38**	62.3	98	0.33	41.7	76	0.37	23.0	88	0.26	32.2	63	0.35	**8.9**
	2	54	80	0.14	22.4	94	0.21	33.2	114	0.21	53.2	96	0.27	35.6	73	0.12	14.3	79	**0.36**	22.1	62	0.05	**4.9**
	3	64	83	0.21	22.0	99	**0.25**	32.1	120	0.24	53.2	102	0.19	34.5	77	0.24	14.5	88	0.09	20.3	67	0.06	**4.8**
	4	59	88	0.25	26.7	103	**0.32**	35.7	126	0.31	57.1	103	**0.32**	37.6	82	0.25	19.5	83	0.10	24.2	64	0.26	**5.4**
WAL	1	66	77	0.26	16.1	90	**0.33**	23.9	108	0.32	43.9	103	0.25	32.8	65	0.24	**0.7**	92	0.04	17.9	59	0.10	5.9
	2	58	83	0.08	24.0	98	0.14	31.8	119	0.13	52.5	106	**0.15**	45.5	71	0.06	6.9	97	-0.09	28.9	63	0.08	**1.7**
WFJ	1	83	79	0.08	8.0	94	**0.10**	**2.1**	113	**0.10**	17.6	106	0.00	19.1	63	0.09	34.6	89	0.01	2.7	70	-0.03	14.6